

The Mutual Awakening Hypothesis: Recursive Collapse, Entropy Stabilization, and Quantum Learning

Khaled Bouzaiene
khaledbouzaiene365@gmail.com

Abstract

The Mutual Awakening Hypothesis (MAH) posits that quantum collapse is an intrinsic, recursive, entropy-stabilizing process driven by internally driven, iterative, nonlinear feedback, potentially operating on quantum amplitudes, thus eliminating the need for an external observer or specific measurement postulate. Through this feedback, a quantum system transitions from superposition towards a definite state, reducing Shannon entropy. We formalize aspects of this using a nonlinear recursive operator acting on probabilities (for illustration and applications) and explore more fundamental dynamics via simulations operating directly on quantum state vectors and density matrices. These simulations validate core MAH tenets: intrinsic collapse emergence, entanglement evolution under local feedback (within model limitations), interplay with decoherence, and parameter dependence. The hypothesis inspires gradient-free quantum learning algorithms and suggests alternatives to conventional AI mechanisms like softmax. Our results point towards a potential unified framework connecting quantum measurement, thermodynamics, and learning, with implications for quantum foundations, decoherence studies, NISQ computation, and AI.

Contents

1	Introduction	1
2	Theoretical Framework: Recursive Collapse Dynamics	2
2.1	Core Concept: Recursive Feedback	2
2.2	Simplified Model: Recursive Probability Operator	2
2.3	Entropy Stabilization	2
2.4	Connections to Learning and AI	3
3	Experimental Validation of Collapse Dynamics	3
3.1	Objectives	3
3.2	Experiment 1: Collapse from a Uniform Superposition (Probability Model)	3
3.2.1	Objective	3
3.2.2	Setup	4
3.2.3	Algorithm	4
3.2.4	Results	4
3.2.5	Analysis	5
3.3	Experiment 2: Locality Test on an Entangled Bell State (Probability Model - Revised)	5
3.3.1	Objective	5
3.3.2	Setup	5
3.3.3	Algorithm	5
3.3.4	Results	5
3.3.5	Analysis	6
3.4	Experiment 3: Adaptive Collapse Dynamics (Probability Model)	6
3.4.1	Objective	6
3.4.2	Setup	6
3.4.3	Algorithm	7
3.4.4	Results	7
3.4.5	Analysis	8
3.5	Experiment 4: Collapse via Internal Feedback (Probability Model - Self-Organized Instability)	8
3.5.1	Objective	8
3.5.2	Setup	8
3.5.3	Algorithm	8
3.5.4	Results	8
3.5.5	Analysis	9
3.6	Experiment 5: Amplitude Feedback and Self-Reinforcing Collapse (Amplitude Model)	9
3.6.1	Objective	9
3.6.2	Mechanism	9
3.6.3	Algorithm	10
3.6.4	Results	10
3.6.5	Interpretation	10
3.7	Experiment 6: Entanglement Evolution Under Feedback (Density Matrix Model)	10
3.7.1	Objective	10
3.7.2	Mechanism	11
3.7.3	Algorithm	11

3.7.4	Results	11
3.7.5	Interpretation	12
3.8	Experiment 7: Decoherence Versus Feedback Interplay (Density Matrix Model)	12
3.8.1	Objective	12
3.8.2	Mechanism	12
3.8.3	Algorithm	13
3.8.4	Results	13
3.8.5	Interpretation	13
3.9	Experiment 8: Parameter Sweep on Feedback Strength (Amplitude Model)	14
3.9.1	Objective	14
3.9.2	Mechanism	14
3.9.3	Algorithm	15
3.9.4	Results	15
3.9.5	Interpretation	16
4	Quantum-Inspired Learning via Recursive Collapse (Using Eq. 2)	16
4.1	Objective	16
4.2	Model: Recursive Classification	16
4.3	Simulation: Binary Classification	17
4.3.1	Setup	17
4.3.2	Algorithm	17
4.3.3	Results	17
4.3.4	Analysis	19
4.4	Discussion	19
5	Recursive Amplification in AI: Beyond Softmax (Using Eq. 2)	19
5.1	Motivation and Formulation	19
5.2	Demonstration: Recursive Amplification vs. Softmax	19
5.2.1	Setup	19
5.2.2	Algorithm	20
5.2.3	Results	20
5.2.4	Analysis	21
5.3	Implications for AI	21
6	Discussion and Conclusion	21
6.1	Summary of Hypothesis and Findings	21
6.2	Implications for Quantum Foundations	21
6.3	Implications for Thermodynamics	21
6.4	Implications for Quantum and Classical Computation	22
6.5	Limitations and Future Work	22
	References	24

1 Introduction

Quantum mechanics describes systems existing in superpositions, which seemingly "collapse" to a single outcome upon measurement [11]. Standard interpretations often invoke external observers (Copenhagen) or postulate discontinuous state reduction (*process 1* in [34]). While decoherence explains the rapid decay of interference due to environmental coupling [37, 30], it doesn't fully solve the measurement problem: the emergence of a unique, definite outcome from the post-decoherence mixture, often referred to as the "pointer state" problem [36]. Alternative approaches, such as spontaneous collapse models (e.g., GRW [14], CSL [25], Diosi-Penrose [10, 26]) modify quantum dynamics explicitly [4], whereas interpretational frameworks like Many-Worlds [13] or Bohmian mechanics [8] offer different perspectives without modifying the dynamics but introducing other ontological elements.

The **Mutual Awakening Hypothesis (MAH)** proposes a different view: collapse is an intrinsic, continuous, and recursive process *within* the quantum system. It suggests that collapse arises from internal, nonlinear feedback mechanisms that amplify dominant components (potentially amplitudes) of the state, thereby stabilizing the system's informational (Shannon) entropy by driving it towards a definite state. Within MAH, "collapse" refers primarily to this dynamical process of convergence to a single outcome with minimized entropy, driven by amplification, rather than necessarily the instantaneous projection postulate. This "mutual awakening" signifies a self-organization process, analogous to phenomena in systems far from equilibrium studied in synergetics [17, 18], where the system's components iteratively co-determine the final outcome.

This paper explores MAH by addressing key questions:

- 1. What drives quantum collapse?** We propose nonlinear recursive feedback acting potentially on quantum amplitudes as a driver, leading towards a single outcome and entropy reduction. We utilize a simplified probability-level recursive operator (Eq. 2) for illustration and computational modeling.
- 2. How does it maintain physical consistency?** We present simulations suggesting the mechanism respects locality constraints (within the model's scope), consistent with no-signaling principles [5, 3, 15], when acting on entangled systems and investigate its interaction with environmental decoherence.
- 3. Can it inspire computational paradigms?** The recursive dynamics motivate novel approaches for gradient-free quantum-inspired learning [7, 31] and alternatives to functions like softmax in classical AI attention mechanisms [33].

This paper is structured as follows:

- Section 2: Outlines the theoretical framework, including the core concept of recursive feedback and the simplified probability-level recursive operator (Eq. 2).
- Section 3: Presents experimental simulations. It starts with illustrative examples using the probability operator (Sec 3.2-3.5) and then details simulations operating on quantum amplitudes and density matrices (Sec 3.6-3.9), examining collapse, entanglement, decoherence, and parameter sensitivity. Algorithms replace code. Figures are integrated.
- Section 4: Demonstrates a practical quantum-inspired, gradient-free classification algorithm based on the recursive probability operator.
- Section 5: Explores the recursive operator as an iterative alternative to softmax in AI.
- Section 6: Discusses the broader implications, limitations, and future research directions.

2 Theoretical Framework: Recursive Collapse Dynamics

MAH models collapse as an intrinsic, recursive, entropy-stabilizing process driven by feedback amplification.

2.1 Core Concept: Recursive Feedback

Fundamentally, MAH posits that the collapse dynamic involves a nonlinear feedback loop where components of the quantum state associated with larger probabilities are iteratively reinforced. This could operate directly on amplitudes $\alpha_i(t)$ in $|\psi(t)\rangle = \sum_i \alpha_i(t)|i\rangle$, potentially involving phase adjustments, or be modeled at the level of probabilities $P_i(t) = |\alpha_i(t)|^2$. The key is the recursive amplification of dominant components, differing from linear Schrödinger evolution but potentially drawing conceptual parallels to nonlinear modifications explored in objective collapse models [4] or nonlinear wave mechanics [6], although MAH proposes a distinct feedback mechanism rather than a direct modification of the evolution equation itself. A conceptual form for amplitude feedback (explored computationally in Sec 3.6) might be:

$$\alpha_i(t+1) \propto \alpha_i(t) \cdot f(\{|\alpha_j(t)|^2\}) \quad (1)$$

where f is a function that increases with the probability $|\alpha_i(t)|^2$ relative to others, followed by normalization.

2.2 Simplified Model: Recursive Probability Operator

For illustrative purposes and for building practical inspired algorithms (Sec 4, 5), we often work with a simplified model operating directly on probabilities. The evolution is governed by the nonlinear recursive operator:

$$P_i^{(t+1)} = \frac{(P_i^{(t)} + b_i)^k}{\sum_j (P_j^{(t)} + b_j)^k} \quad (2)$$

where:

- $P_i^{(t)}$ is the probability of state $|i\rangle$ at iteration t .
- $b_i \geq 0$ are small biases (modeling asymmetries, fluctuations, or adaptive feedback signals).
- $k > 1$ is an amplification exponent capturing the feedback strength.
- Normalization ensures $\sum_i P_i^{(t+1)} = 1$.

This operator captures the essence of MAH – amplification of dominant components leading to collapse – in a mathematically tractable form, resembling iterative update rules seen in competitive learning or winner-take-all networks [29].

2.3 Entropy Stabilization

Regardless of the specific level of the feedback mechanism (amplitude or probability), the concentration of the state onto a single outcome leads to a reduction in the Shannon entropy [32]. For a quantum state described by a density matrix ρ , the von Neumann entropy $S(\rho) = -\text{Tr}(\rho \log_2 \rho)$ [34, 35, 24] is a more general measure of mixedness or uncertainty. The reduction towards a pure

state corresponds to entropy minimization. Here, we primarily use Shannon entropy of the diagonal elements (probabilities) in a chosen basis:

$$S(t) = - \sum_i P_i(t) \log_2 P_i(t) \quad (3)$$

where $P_i(t) = |\alpha_i(t)|^2$ (or is directly the probability from Eq. 2). As the system collapses, $S(t)$ decreases, reflecting self-organization towards a state of minimal informational uncertainty, a concept explored in complexity and information dynamics [28].

2.4 Connections to Learning and AI

The recursive feedback principle extends naturally:

- **QML:** Adaptive feedback mechanisms operating on probabilities (Eq. 2) can drive learning without explicit gradients (Sec 4), relevant for quantum machine learning approaches [7, 31] and potentially useful for variational quantum algorithms [9] on NISQ devices [27]. Conceptual amplitude-level feedback offers further possibilities.
- **AI:** Iterative application of Eq. 2 offers an alternative to single-shot transformations like softmax [16], particularly in contexts like attention mechanisms [33], allowing dynamic control over distribution sharpness (Sec 5). This iterative refinement resonates with concepts in recurrent neural networks [12].

Note: A detailed glossary or appendix of notation could be beneficial for readers less familiar with the combined quantum and computational terminology in a longer exposition.

3 Experimental Validation of Collapse Dynamics

We conducted simulations to test MAH, starting with the simplified probability operator (Eq. 2) and progressing to simulations operating directly on quantum states.

3.1 Objectives

1. Illustrate basic collapse dynamics (bias-driven, adaptive, self-organized) using the probability model (Eq. 2).
2. Test locality propagation in the probability model for an entangled state.
3. Demonstrate collapse dynamics via direct amplitude feedback simulation.
4. Investigate entanglement evolution under local feedback within the amplitude/density matrix formalism.
5. Study the interplay between MAH feedback and environmental decoherence.
6. Analyze the impact of feedback strength parameters in amplitude models.

— Probability Operator Simulations (Eq. 2) —

3.2 Experiment 1: Collapse from a Uniform Superposition (Probability Model)

3.2.1 Objective

Verify bias-driven collapse and entropy reduction using Eq. 2.

3.2.2 Setup

A system with 4 basis states, initially in a uniform superposition ($P = [0.25, 0.25, 0.25, 0.25]$). A small constant bias $b = [0.02, 0, 0, 0]$ favoring state $|00\rangle$ is applied. $k = 2.0$.

3.2.3 Algorithm

Algorithm 1 Exp1 (Prob): Bias-driven collapse simulation.

Require: Initial probabilities P_{init} , bias vector b , exponent k , iterations N_{iters} .

Ensure: History of probabilities P_{hist} , History of entropy S_{hist} .

```

1: Initialize  $P \leftarrow P_{init}$ 
2: Initialize empty lists  $P_{hist}, S_{hist}$ 
3: for  $t = 0$  to  $N_{iters}$  do
4:   Append  $P$  to  $P_{hist}$ 
5:   Calculate  $S \leftarrow -\sum_i P_i \log_2(P_i + \epsilon)$   $\triangleright \epsilon \approx 10^{-12}$ 
6:   Append  $S$  to  $S_{hist}$ 
7:   if  $t < N_{iters}$  then
8:     Calculate Numerator  $N_i \leftarrow (P_i + b_i)^k$  for all  $i$ 
9:     Calculate Denominator  $D \leftarrow \sum_j N_j$ 
10:    if  $D > 0$  then
11:       $P_i \leftarrow N_i/D$  for all  $i$ 
12:    else
13:       $P_i \leftarrow 1/\dim(P)$  for all  $i$ 
14:    end if
15:  end if
16: end for
17: return  $P_{hist}, S_{hist}$ 

```

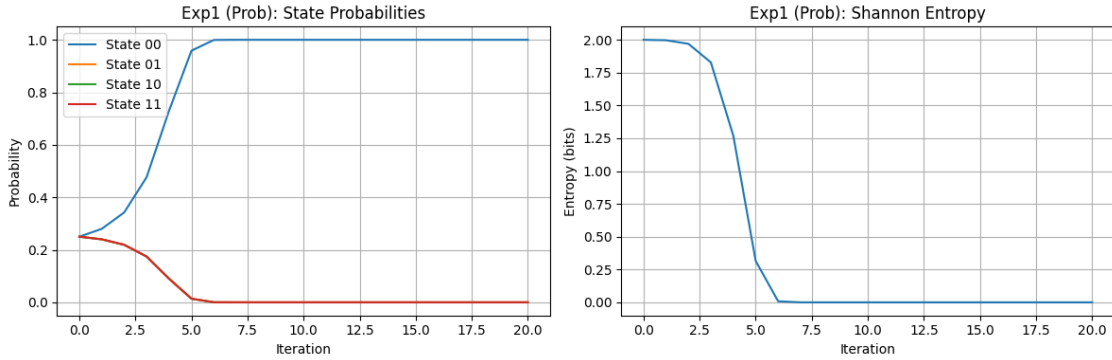


Figure 1: Results of Exp1 (Prob): Bias-driven collapse and entropy reduction. Left: State probabilities over iterations. Right: Shannon entropy (bits) over iterations.

3.2.4 Results

The probability of the biased state ($|00\rangle$) rapidly approaches 1.0 (~ 7 iterations). Shannon entropy monotonically decreases from 2.0 bits to nearly 0 bits (Fig. 1).

3.2.5 Analysis

Confirms Eq. 2 effectively induces deterministic collapse driven by a small initial asymmetry, validating the basic amplification and entropy stabilization aspects of MAH in this model.

3.3 Experiment 2: Locality Test on an Entangled Bell State (Probability Model - Revised)

3.3.1 Objective

Assess whether applying Eq. 2 *locally* to one qubit of an entangled pair (modeled via probabilities) violates locality (no-signaling) by instantaneously affecting the marginal probabilities of the other qubit, consistent with Bell's theorem analyses [5].

3.3.2 Setup

Consider the Bell state $|\psi\rangle = (|00\rangle + |11\rangle)/\sqrt{2}$. The joint probability distribution is $P_{joint} = [P_{00}, P_{01}, P_{10}, P_{11}] = [0.5, 0, 0, 0.5]$. We apply a bias b_A favoring state $|0\rangle$ for qubit A. This bias affects the joint states $|00\rangle$ and $|01\rangle$. So, the bias vector for the joint system is $b_{joint} = [b_A, b_A, 0, 0]$. We use $b_A = 0.01$, $k = 2.0$, $N_{iters} = 10$. We monitor the marginal probabilities $P_A = [P_{00} + P_{01}, P_{10} + P_{11}]$ and $P_B = [P_{00} + P_{10}, P_{01} + P_{11}]$.

3.3.3 Algorithm

Algorithm 2 Exp2 (Prob): Locality test on Bell state probabilities.

Require: Initial joint probabilities $P_{joint,init}$, local bias $b_{A,local}$, exponent k , iterations N_{iters} .

Ensure: Evolution of marginal probabilities $P_A(t)$ and $P_B(t)$.

```

1: Initialize  $P_{joint} \leftarrow P_{joint,init}$ 
2: Initialize  $b_{joint} \leftarrow [b_{A,local}, b_{A,local}, 0, 0]$ 
3: for  $t = 0$  to  $N_{iters}$  do
4:   Calculate  $P_A \leftarrow [P_{joint,0} + P_{joint,1}, P_{joint,2} + P_{joint,3}]$ 
5:   Calculate  $P_B \leftarrow [P_{joint,0} + P_{joint,2}, P_{joint,1} + P_{joint,3}]$ 
6:   Print  $t, P_A, P_B, P_{joint}$ 
7:   if  $t < N_{iters}$  then
8:     Calculate Numerator  $N_i \leftarrow (P_{joint,i} + b_{joint,i})^k$  for  $i = 0..3$ 
9:     Calculate Denominator  $D \leftarrow \sum_j N_j$ 
10:    if  $D > 0$  then
11:       $P_{joint,i} \leftarrow N_i/D$  for all  $i$ 
12:    else
13:       $P_{joint,i} \leftarrow 1/4$  for all  $i$ 
14:    end if
15:  end if
16: end for

```

3.3.4 Results

As the local bias on qubit A amplifies the $|00\rangle$ component, the $|11\rangle$ component decreases due to normalization. Consequently, P_A shifts towards $[1, 0]$. Because $|00\rangle$ contributes to $P_B[0]$ and

$|11\rangle$ contributes to $P_B[1]$, P_B also shifts towards $[1,0]$, mirroring P_A . (No figure provided for this experiment).

3.3.5 Analysis

Within this probability-based model (Eq. 2 applied to the joint distribution), a local bias instantaneously affects the partner’s marginal distribution. This change reflects the pre-existing correlations inherent in the entangled state’s probability distribution and does not imply the possibility of faster-than-light signaling, in accordance with established principles of quantum mechanics [5, 3, 15]. A deeper analysis needs a full quantum state framework (see Exp 3.7).

3.4 Experiment 3: Adaptive Collapse Dynamics (Probability Model)

3.4.1 Objective

Demonstrate selection/classification using Eq. 2 with an adaptive bias derived from a target state.

3.4.2 Setup

4 classes, $P_{init} = [0.25, 0.25, 0.25, 0.25]$. Target class 2 ($|10\rangle$), $target = [0, 0, 1, 0]$. Adaptive bias $b = \eta \times (target - P)$ (using clamping interpretation: $base = \max(0, P + b)$), $\eta = 0.1$, $k = 2.0$. Track target probability $P_{target} = P_2$ and pseudo-loss $-\log(P_{target})$.

3.4.3 Algorithm

Algorithm 3 Exp3 (Prob): Adaptive collapse simulation.

Require: Initial probabilities P_{init} , target vector T , bias rate η , exponent k , iterations N_{iters} .

Ensure: History of target probability $P_{target,hist}$, History of pseudo-loss L_{hist} .

```

1: Initialize  $P \leftarrow P_{init}$ 
2: Initialize empty lists  $P_{target,hist}$ ,  $L_{hist}$ 
3: for  $t = 0$  to  $N_{iters}$  do
4:    $p_{target} \leftarrow P_2$  ▷ Target index assumed 2
5:   Append  $p_{target}$  to  $P_{target,hist}$ 
6:    $L \leftarrow -\log(p_{target} + \epsilon)$ 
7:   Append  $L$  to  $L_{hist}$ 
8:   Print  $t, p_{target}, L$ 
9:   if  $t < N_{iters}$  then
10:     $b_{adaptive} \leftarrow \eta \times (T - P)$ 
11:    Calculate Base  $B_i \leftarrow P_i + b_{adaptive,i}$  for all  $i$ 
12:    Calculate Clamped Base  $B'_i \leftarrow \max(0, B_i)$ 
13:    Calculate Numerator  $N_i \leftarrow (B'_i)^k$ 
14:    Calculate Denominator  $D \leftarrow \sum_j N_j$ 
15:    if  $D > 0$  then
16:       $P_i \leftarrow N_i/D$  for all  $i$ 
17:    else
18:       $P_i \leftarrow 1/\dim(P)$  for all  $i$ 
19:    end if
20:  end if
21: end for
22: return  $P_{target,hist}$ ,  $L_{hist}$ 

```

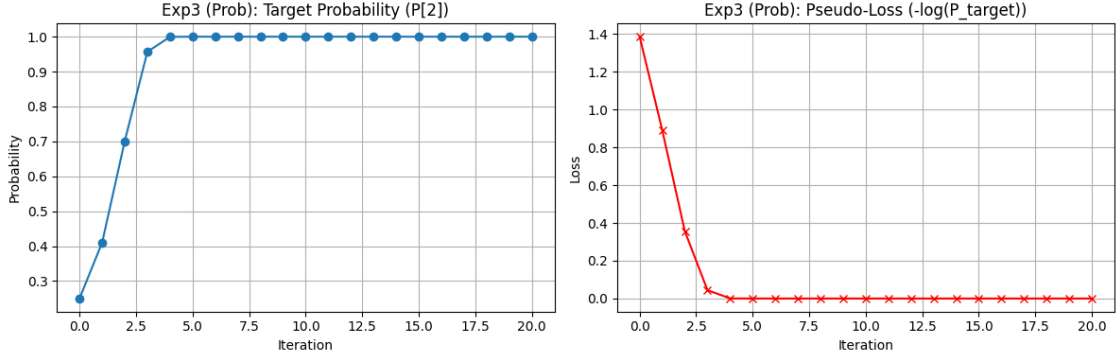


Figure 2: Results of Exp3 (Prob): Adaptive collapse dynamics. Left: Target state probability (P_2) over iterations. Right: Pseudo-loss ($-\log P_2$) over iterations.

3.4.4 Results

Target state probability ($|10\rangle$) approaches 1.0 (~ 6 iterations). Pseudo-loss drops from ~ 1.386 to near 0 (Fig. 2).

3.4.5 Analysis

Demonstrates Eq. 2 can function as a selection process driven by an error signal (difference from target), guiding the collapse effectively towards the desired outcome. This visually confirms (Fig. 2) the convergence mimicks optimization without explicit gradient calculation.

3.5 Experiment 4: Collapse via Internal Feedback (Probability Model - Self-Organized Instability)

3.5.1 Objective

Evaluate if collapse can emerge using Eq. 2 from internal reinforcement alone, without a pre-defined external bias.

3.5.2 Setup

Uniform initial state $P = [0.25, 0.25, 0.25, 0.25]$. At each step, a small positive bias ('boost = 0.01') is added *only* to the state that currently has the maximum probability. $k = 2.0$.

3.5.3 Algorithm

Algorithm 4 Exp4 (Prob): Self-organized collapse simulation.

Require: Initial probabilities P_{init} , boost value b_{boost} , exponent k , iterations N_{iters} .

Ensure: History of probabilities P_{hist} .

```
1: Initialize  $P \leftarrow P_{init}$ 
2: Initialize empty list  $P_{hist}$ 
3: for  $t = 0$  to  $N_{iters}$  do
4:   Append  $P$  to  $P_{hist}$ 
5:   Print  $t, P$ 
6:   if  $t < N_{iters}$  then
7:     Find index  $i^* = \arg \max_j P_j$ 
8:     Initialize bias vector  $b \leftarrow \mathbf{0}$ 
9:      $b_{i^*} \leftarrow b_{boost}$ 
10:    Calculate Numerator  $N_i \leftarrow (P_i + b_i)^k$  for all  $i$ 
11:    Calculate Denominator  $D \leftarrow \sum_j N_j$ 
12:    if  $D > 0$  then
13:       $P_i \leftarrow N_i/D$  for all  $i$ 
14:    else
15:       $P_i \leftarrow 1/\dim(P)$  for all  $i$ 
16:    end if
17:  end if
18: end for
19: return  $P_{hist}$ 
```

3.5.4 Results

Even starting uniform, the internal feedback loop amplifies tiny numerical differences, rapidly collapsing the system to a single, effectively randomly chosen state (~ 7 -8 iterations) (Fig. 3).

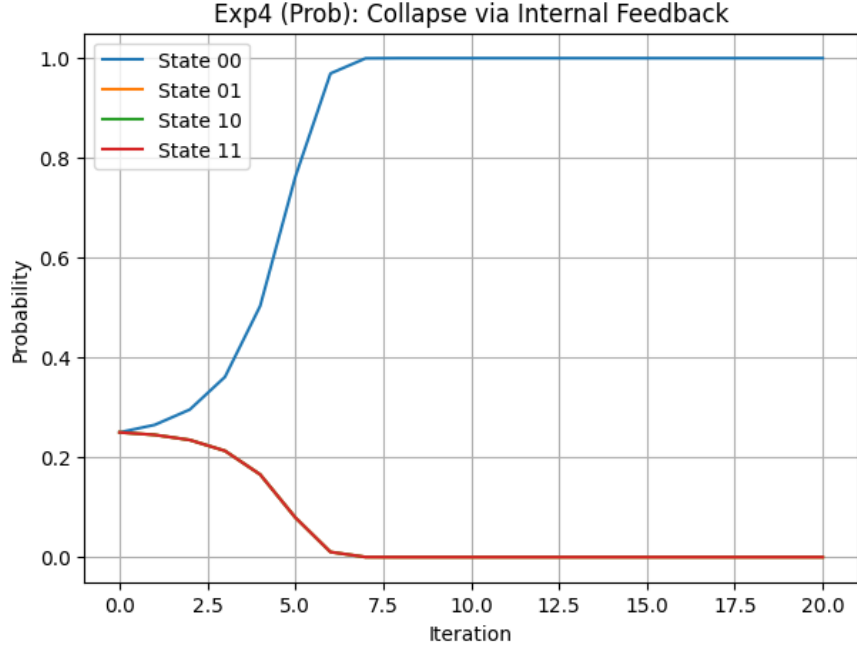


Figure 3: Results of Exp4 (Prob): Self-organized collapse via internal feedback. Shows probabilities of the four states evolving over iterations, with one randomly selected state reaching probability 1.

3.5.5 Analysis

Confirms the inherent instability in the recursive dynamic (Eq. 2). Figure 3 visually demonstrates how internal reinforcement of fluctuations suffices to break symmetry and drive collapse without external bias, supporting the MAH premise of self-organization [18].

— Amplitude/Density Matrix Simulations —

These simulations operate directly on quantum state vectors $|\psi\rangle$ or density matrices ρ , providing a more quantum-native exploration of MAH concepts.

General Utilities

(Assume standard functions: ‘normalize(v)’ for vector normalization, ‘entropy(probs, base=2)’ for Shannon entropy.)

3.6 Experiment 5: Amplitude Feedback and Self-Reinforcing Collapse (Amplitude Model)

3.6.1 Objective

Model collapse as recursive amplification of the dominant amplitude.

3.6.2 Mechanism

Internal feedback on amplitudes ψ_i . Identify $i^* = \arg \max |\psi_i|^2$. Apply $\psi_{i^*} \leftarrow \gamma \cdot \psi_{i^*}$. Optionally align phases: $\psi \leftarrow \psi \cdot e^{-i \arg(\psi_{i^*})}$. Normalize ψ . No decoherence. $\gamma = 1.1$. Initial state ψ represents

uniform superposition magnitudes.

3.6.3 Algorithm

Algorithm 5 Exp5: Amplitude feedback collapse simulation.

Require: Initial state ψ_{init} , feedback gain γ , iterations N_{iters} , boolean $align_phases$.

Ensure: Log of (step, probabilities, entropy) tuples $Logs$.

```

1: Initialize  $\psi \leftarrow \psi_{init}$ 
2: Initialize empty list  $Logs$ 
3: for  $t = 0$  to  $N_{iters}$  do
4:   Calculate  $P_i \leftarrow |\psi_i|^2$  for all  $i$ 
5:   Calculate  $S \leftarrow -\sum_i P_i \log_2(P_i + \epsilon)$ 
6:   Append  $(t, P, S)$  to  $Logs$ 
7:   Print  $t, P, S$ 
8:   if  $S < \epsilon_{conv}$  or  $t == N_{iters}$  then                                ▷ Stop if converged or last step
9:     break
10:  end if
11:  Find index  $i^* = \arg \max_j P_j$ 
12:   $\psi_{i^*} \leftarrow \gamma \cdot \psi_{i^*}$ 
13:  if  $align\_phases$  then
14:     $\phi^* \leftarrow \text{angle}(\psi_{i^*})$ 
15:     $\psi \leftarrow \psi \cdot e^{-i\phi^*}$ 
16:  end if
17:   $\psi \leftarrow \text{normalize}(\psi)$ 
18: end for
19: return  $Logs$ 

```

3.6.4 Results

System entropy drops rapidly from ~ 2.0 bits towards 0 within ~ 10 steps as probabilities concentrate on one state (Similar entropy profile to the $\gamma = 1.1$ curve in Fig. 4).

3.6.5 Interpretation

Confirms that collapse can emerge from a nonlinear, amplitude-based feedback mechanism without external observation or explicit environmental noise, supporting the core MAH concept at the state vector level.

3.7 Experiment 6: Entanglement Evolution Under Feedback (Density Matrix Model)

3.7.1 Objective

Explore entanglement evolution in a Bell state under local amplitude feedback applied via the reduced density matrix.

3.7.2 Mechanism

Start with Bell state $|\psi\rangle = (|00\rangle + |11\rangle)/\sqrt{2}$. Calculate $\rho = |\psi\rangle\langle\psi|$, then reduced state $\rho_A = \text{Tr}_B(\rho)$. Get probabilities $p_A = \text{diag}(\rho_A)$. Apply feedback $p_{A,i^*} \leftarrow \gamma \cdot p_{A,i^*}$ where $i^* = \arg \max p_A$. Normalize p_A . Construct a local operator $U = \text{diag}(\sqrt{p_A})$. Apply $|\psi_{new}\rangle = (U \otimes I)|\psi\rangle$. Normalize $|\psi_{new}\rangle$. $\gamma = 1.1$. *(Disclaimer: This specific update rule using $U = \text{diag}(\sqrt{p_A})$ is exploratory and currently lacks rigorous physical justification. It serves to illustrate how local feedback based on reduced state properties *could* influence the global state dynamically).*

3.7.3 Algorithm

Algorithm 6 Exp6: Entanglement evolution under local feedback.

Require: Initial Bell state ψ_{init} , feedback gain γ , iterations N_{iters} .

Ensure: Log of (step, joint probabilities, entropy) tuples $Logs$.

```

1: Initialize  $\psi \leftarrow \psi_{init}$ 
2: Initialize  $I \leftarrow \text{Identity}(2)$ 
3: Initialize empty list  $Logs$ 
4: for  $t = 0$  to  $N_{iters}$  do
5:   Calculate  $P_{joint,i} \leftarrow |\psi_i|^2$  for all  $i$ 
6:   Calculate  $S \leftarrow -\sum_i P_{joint,i} \log_2(P_{joint,i} + \epsilon)$ 
7:   Append  $(t, P_{joint}, S)$  to  $Logs$ 
8:   Print  $t, P_{joint}, S$ 
9:   if  $S < \epsilon_{conv}$  or  $t == N_{iters}$  then
10:    break
11:   end if
12:    $\rho \leftarrow |\psi\rangle\langle\psi|$ 
13:    $\rho_A \leftarrow \text{Tr}_B(\rho)$  ▷ Partial trace over subsystem B
14:    $p_A \leftarrow \text{diag}(\text{Re}(\rho_A))$ 
15:   if  $\sum p_A > \epsilon_{norm}$  then
16:      $i^* = \arg \max p_A$ 
17:      $p_{A,i^*} \leftarrow \gamma \cdot p_{A,i^*}$ 
18:      $p_A \leftarrow p_A / \sum p_A$ 
19:   else
20:      $p_A \leftarrow [0.5, 0.5]$ 
21:   end if
22:    $U \leftarrow \text{diag}(\sqrt{\max(0, p_A)})$  ▷ Construct local operator (Exploratory)
23:    $\psi \leftarrow (U \otimes I)\psi$  ▷ Apply local op on A
24:    $\psi \leftarrow \text{normalize}(\psi)$ 
25: end for
26: return  $Logs$ 

```

3.7.4 Results

Entropy decays exponentially. The state evolves, reflecting changes driven by local feedback on subsystem A propagating through the entanglement. (No figure provided for this experiment).

3.7.5 Interpretation

This simulation models how local feedback, acting via the reduced state, affects the global entangled state. Within the constraints of the specific update rule chosen, it shows entanglement evolving dynamically. It respects locality in the sense that the feedback *rule* is based on local properties ρ_A , but the *effect* is global due to entanglement. The model suggests entanglement decay could be a process, not a jump, aligning with statistical observations. The validity depends heavily on justifying the specific form of the feedback operator $U \otimes I$.

3.8 Experiment 7: Decoherence Versus Feedback Interplay (Density Matrix Model)

3.8.1 Objective

Introduce environmental noise (decoherence) alongside amplitude feedback, simulating concepts from decoherence theory [37, 30].

3.8.2 Mechanism

Start with uniform ψ . Apply amplitude feedback $\psi_{i^*} \leftarrow \gamma \cdot \psi_{i^*}$ ($\gamma = 1.1$). Construct $\rho = |\psi\rangle\langle\psi|$. Apply decoherence by damping off-diagonals: $\rho \leftarrow (1-r)\rho + r \cdot \text{diag}(\text{diag}(\rho))$, where r is decoherence rate (0.05). Extract dominant eigenvector of the decohered ρ as the new ψ . Normalize.

3.8.3 Algorithm

Algorithm 7 Exp7: Simulation of feedback vs decoherence.

Require: Initial state ψ_{init} , feedback gain γ , decoherence rate r , iterations N_{iters} .

Ensure: Log of (step, probabilities, entropy) tuples $Logs$.

```

1: Initialize  $\psi \leftarrow \psi_{init}$ 
2: Initialize empty list  $Logs$ 
3: for  $t = 0$  to  $N_{iters}$  do
4:   Calculate  $P_i \leftarrow |\psi_i|^2$  for all  $i$ 
5:   Calculate  $S \leftarrow -\sum_i P_i \log_2(P_i + \epsilon)$ 
6:   Append  $(t, P, S)$  to  $Logs$ 
7:   Print  $t, P, S$ 
8:   if  $S < \epsilon_{conv}$  or  $t == N_{iters}$  then
9:     break
10:  end if
11:  if  $\|\psi\| > \epsilon_{norm}$  then
12:     $i^* = \arg \max P_i$ 
13:     $\psi_{i^*} \leftarrow \gamma \cdot \psi_{i^*}$ 
14:     $\psi \leftarrow \text{normalize}(\psi)$ 
15:  else
16:    break ▷ Psi vector became zero
17:  end if
18:   $\rho \leftarrow |\psi\rangle\langle\psi|$ 
19:   $\rho_{diag} \leftarrow \text{diag}(\text{diag}(\rho))$  ▷ Get diagonal elements
20:   $\rho_{decohered} \leftarrow (1 - r)\rho + r\rho_{diag}$  ▷ Apply damping
21:   $\rho_{decohered} \leftarrow (\rho_{decohered} + \rho_{decohered}^\dagger)/2$  ▷ Ensure Hermitian
22:  Eigenvalues  $\lambda$ , Eigenvectors  $V \leftarrow \text{eigh}(\rho_{decohered})$ 
23:   $\psi \leftarrow V_{:,last}$  ▷ Dominant eigenvector
24:   $\psi \leftarrow \text{normalize}(\psi)$ 
25: end for
26: return  $Logs$ 

```

3.8.4 Results

Collapse still occurs, driving entropy towards zero, but the process is slower compared to pure amplitude feedback (Exp 3.6). (No figure provided for this experiment).

3.8.5 Interpretation

Feedback-driven collapse (MAH mechanism) is robust to moderate environmental decoherence. Decoherence (damping interference) and MAH feedback (selection/amplification) appear as distinct but interacting processes. Decoherence primarily removes off-diagonal terms, turning a pure superposition into a mixed state (diagonal density matrix in the pointer basis [36]), while MAH provides the subsequent *selection mechanism* that picks one component from that mixture and amplifies it to probability 1.

3.9 Experiment 8: Parameter Sweep on Feedback Strength (Amplitude Model)

3.9.1 Objective

Explore the impact of internal amplification strength γ on collapse dynamics.

3.9.2 Mechanism

Run the amplitude feedback simulation (Exp 3.6) for various γ values (e.g., 1.01, 1.05, 1.1, 1.2). Track entropy evolution for each γ .

3.9.3 Algorithm

Algorithm 8 Exp8: Parameter sweep for feedback strength gamma.

Require: Initial state ψ_{init} , list of γ values Γ_{list} , iterations N_{iters} , boolean *align_phases*.

Ensure: Dictionary *All_Logs* mapping each γ to its Log.

```

1: Initialize empty dictionary All_Logs  $\gamma \in \Gamma_{list}$ 
2: Initialize  $\psi \leftarrow \psi_{init}$ 
3: Initialize empty list Logs
4: for  $t = 0$  to  $N_{iters}$  do
5:   Calculate  $P_i \leftarrow |\psi_i|^2$  for all  $i$ 
6:   Calculate  $S \leftarrow -\sum_i P_i \log_2(P_i + \epsilon)$ 
7:   Append  $(t, P, S)$  to Logs
8:   if  $S < \epsilon_{conv}$  or  $t == N_{iters}$  then
9:     if  $S < \epsilon_{conv}$  and  $t < N_{iters}$  then ▷ Fill logs if converged early
10:       $final\_entry \leftarrow Logs[-1]$ 
11:      for  $fill\_t = t + 1$  to  $N_{iters}$  do
12:        Append  $final\_entry$  to Logs
13:      end for
14:    end if
15:    break
16:   end if
17:   if  $\|\psi\| > \epsilon_{norm}$  then
18:      $i^* = \arg \max P_i$ 
19:      $\psi_{i^*} \leftarrow \gamma \cdot \psi_{i^*}$ 
20:     if align_phases then
21:        $\phi^* \leftarrow \text{angle}(\psi_{i^*})$ 
22:        $\psi \leftarrow \psi \cdot e^{-i\phi^*}$ 
23:     end if
24:      $\psi \leftarrow \text{normalize}(\psi)$ 
25:   else ▷ Handle zero vector
26:      $final\_entry \leftarrow Logs[-1]$ 
27:     for  $fill\_t = t + 1$  to  $N_{iters}$  do
28:       Append  $final\_entry$  to Logs
29:     end for
30:     break
31:   end if
32: end for
33:  $All\_Logs[\gamma] \leftarrow Logs$ 
34:
35: return All_Logs

```

3.9.4 Results

Stronger γ leads to faster collapse (steeper entropy decrease). Very low γ (~ 1) results in slow collapse, as clearly visible for $\gamma = 1.01$ compared to $\gamma = 1.2$ in Fig. 4.

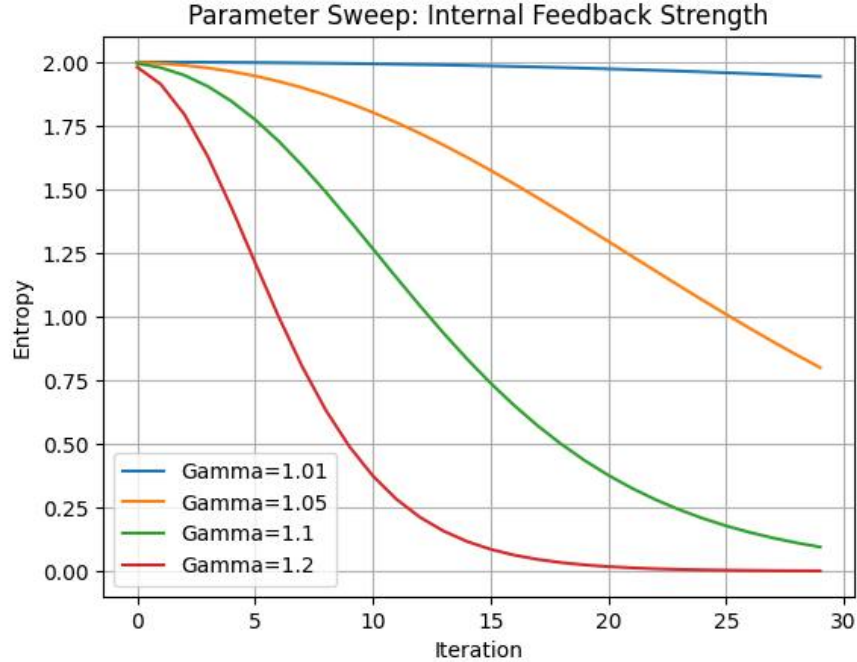


Figure 4: Results of Exp8 (Amp): Parameter sweep for feedback strength γ . Shows entropy evolution (bits) vs iteration for $\gamma \in \{1.01, 1.05, 1.1, 1.2\}$.

3.9.5 Interpretation

The collapse timescale within the MAH amplitude feedback model is directly modulated by the feedback strength γ . This suggests γ (or its equivalent) could be a key physical parameter determining observed collapse rates if MAH is physically realized.

4 Quantum-Inspired Learning via Recursive Collapse (Using Eq. 2)

Building on the adaptive collapse demonstrated in Exp 3.4, we explore the application of the **recursive probability operator (Eq. 2)** as a gradient-free learning mechanism for classical classification tasks, inspired by MAH principles.

4.1 Objective

To demonstrate that the recursive update operator (Eq. 2), applied iteratively to probability vectors encoding input data, can effectively perform classification by driving the system towards a low-entropy state corresponding to the correct class, without calculating gradients.

4.2 Model: Recursive Classification

1. **Encoding:** Map an input data point \mathbf{x} into an initial probability vector $\mathbf{P}^{(0)} = [P_0^{(0)}, \dots, P_{C-1}^{(0)}]$ over C classes based on similarity (e.g., Gaussian kernel vs class centers).

2. **Recursive Refinement:** Apply Eq. 2 for N_{learn_iters} iterations: $P^{(t+1)} \leftarrow \text{Update}(P^{(t)}, \beta, k_{learn})$. Use small constant bias $\beta > 0$.
3. **Classification:** Predict class $\hat{y} = \arg \max_i P_i^{(\text{final})}$.

4.3 Simulation: Binary Classification

4.3.1 Setup

Generate synthetic 2D data from two well-separated Gaussian blobs (classes 0 and 1). Encode each point \mathbf{x} into $\mathbf{P}^{(0)} = [P_0^{(0)}, P_1^{(0)}]$ based on normalized Gaussian similarity to the cluster centers. Apply the recursive operator (Eq. 2) with constant bias $\beta_{learn} = 0.01$ and $k_{learn} = 6$ for $N_{learn_iters} = 15$.

4.3.2 Algorithm

Algorithm 9 Section 4: Quantum-inspired binary classification.

Require: Dataset X (features), Y_{true} (labels), parameters $k_{learn}, \beta_{learn}, N_{learn_iters}$, encoding σ^2 .

Ensure: Predicted labels Y_{pred} , Accuracy acc .

- 1: Calculate class centers $C = [\text{mean}(X[Y_{true} == i]) \text{ for } i \in \text{classes}]$
 - 2: Initialize empty list Y_{pred} data point $\mathbf{x} \in X$
 - 3: Calculate distances $d_i^2 \leftarrow \|\mathbf{x} - C_i\|^2$ for all C_i
 - 4: Calculate similarities $s_i \leftarrow \exp(-d_i^2/\sigma^2)$
 - 5: **if** $\sum s_j < \epsilon_{norm}$ **then**
 - 6: $P_i^{(0)} \leftarrow 1/(\text{classes})$
 - 7: **else**
 - 8: $P_i^{(0)} \leftarrow s_i/\sum s_j$
 - 9: **end if**
 - 10: $P \leftarrow P^{(0)}$
 - 11: **for** $t = 1$ to N_{learn_iters} **do**
 - 12: Calculate $N_i \leftarrow (P_i + \beta_{learn})^{k_{learn}}$
 - 13: $D \leftarrow \sum_j N_j$
 - 14: **if** $D > 0$ **then**
 - 15: $P_i \leftarrow N_i/D$
 - 16: **else**
 - 17: $P_i \leftarrow 1/(\text{classes})$
 - 18: **end if**
 - 19: **end for**
 - 20: $\hat{y} \leftarrow \arg \max_i P_i$
 - 21: Append \hat{y} to Y_{pred}
 - 22:
 - 23: Calculate $acc \leftarrow \text{accuracy_score}(Y_{true}, Y_{pred})$ ▷ Using e.g., sklearn
 - 24: **return** Y_{pred}, acc
-

4.3.3 Results

The simulation typically achieves perfect or near-perfect accuracy (e.g., ‘1.0000’) on this clearly separable dataset (Fig. 5).

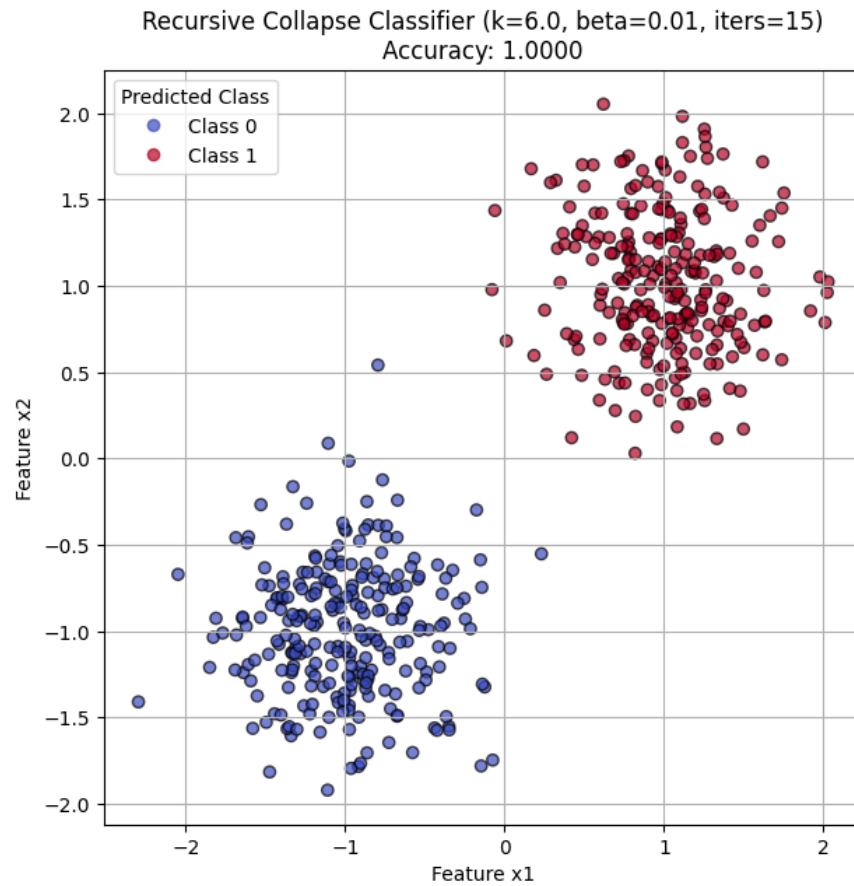


Figure 5: Results of Sec 4: Binary classification using recursive collapse. Scatter plot shows data points colored by predicted class, demonstrating successful separation.

4.3.4 Analysis

This demonstrates that the recursive collapse mechanism (Eq. 2) can function as a computationally lightweight, gradient-free classifier. The classification emerges from the self-organizing dynamics of the operator iteratively refining the initial state encoded from the input data.

4.4 Discussion

This quantum-inspired approach using Eq. 2 offers potential advantages: Gradient-Free, Simplicity, Self-Organization. Its update rule shares conceptual similarities with competitive learning mechanisms like those in Self-Organizing Maps (SOMs) [20], although the normalization and exponent differ. The adaptive bias variant (Exp 3.4) echoes Hebbian learning principles ("neurons that fire together, wire together"). Future work could explore its scalability, performance on complex datasets, adaptive parameter tuning (k, β), and integration into hybrid quantum-classical algorithms [31], potentially within frameworks for variational quantum circuits [9].

5 Recursive Amplification in AI: Beyond Softmax (Using Eq. 2)

The MAH principle of iterative amplification, modeled via **Eq. 2**, can also inform the design of mechanisms in classical AI, offering an alternative to standard functions like Softmax [16].

5.1 Motivation and Formulation

Softmax $P_i = \exp(a_i/T) / \sum_j \exp(a_j/T)$ is a single-step transformation of scores a_i . The recursive operator (Eq. 2), applied iteratively to non-negative transformed scores (e.g., $x_i^{(0)} = \exp(a_i)$), provides an alternative:

$$x_i^{(t+1)} = \frac{(x_i^{(t)} + b)^k}{\sum_j (x_j^{(t)} + b)^k}$$

Key differences: Iterative Refinement, Gradient-Free Dynamics (Post-Scores), Entropy Reduction. This iterative refinement could be relevant for attention mechanisms [33].

5.2 Demonstration: Recursive Amplification vs. Softmax

5.2.1 Setup

Generate random raw scores a . Compute the Softmax distribution $P_{softmax} = \text{softmax}(a)$. Initialize $x^{(0)} = P_{softmax}$. Iterate Eq. 2 with $k = 2.5$, $b = 0.01$ for $N_{amp_iters} = 5$ iterations, starting from $x^{(0)}$. Track distribution $x^{(t)}$ and entropy $S(x^{(t)})$.

5.2.2 Algorithm

Algorithm 10 Section 5: Comparison of Softmax and Recursive Amplification.

Require: Raw scores a , bias b_{amp} , exponent k_{amp} , iterations N_{amp_iters} .

Ensure: Softmax distribution $P_{softmax}$, History of recursive distributions X_{hist} , History of entropies S_{hist} .

```

1:  $P_{softmax} \leftarrow \text{softmax}(a, T = 1)$ 
2:  $S_{softmax} \leftarrow -\sum_i P_{softmax,i} \log_2(P_{softmax,i} + \epsilon)$ 
3: Initialize  $x \leftarrow P_{softmax}$ 
4: Initialize  $X_{hist} \leftarrow [x]$ ,  $S_{hist} \leftarrow [S_{softmax}]$ 
5: for  $t = 1$  to  $N_{amp\_iters}$  do
6:   Calculate  $N_i \leftarrow (x_i + b_{amp})^{k_{amp}}$ 
7:    $D \leftarrow \sum_j N_j$ 
8:   if  $D > 0$  then
9:      $x_i \leftarrow N_i/D$ 
10:  else
11:     $x_i \leftarrow 1/(\text{scores})$ 
12:  end if
13:  Append  $x$  to  $X_{hist}$ 
14:   $S \leftarrow -\sum_i x_i \log_2(x_i + \epsilon)$ 
15:  Append  $S$  to  $S_{hist}$ 
16:  Print  $t, S$ 
17: end for
18: return  $P_{softmax}, X_{hist}, S_{hist}$ 

```

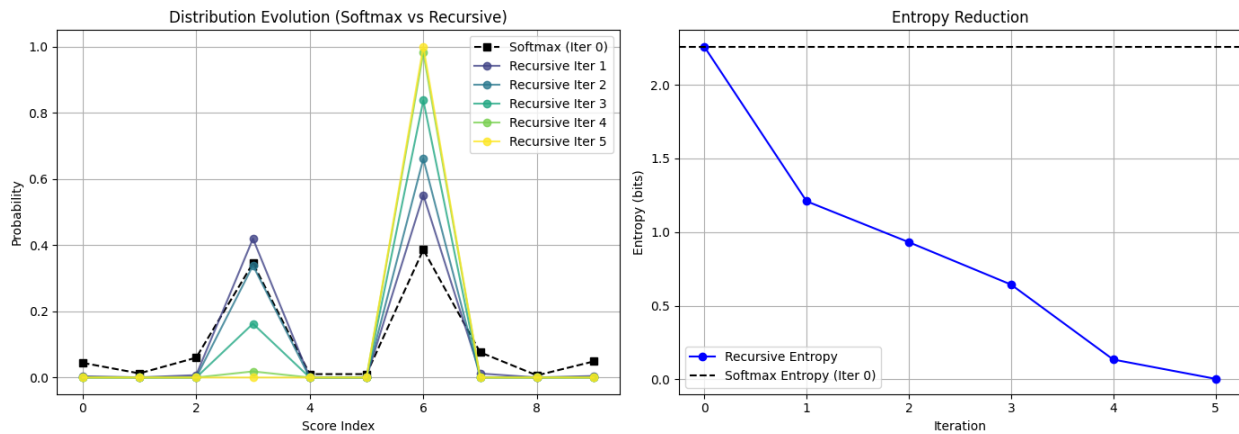


Figure 6: Results of Sec 5: Comparison of Softmax and iterative recursive amplification. Left: Distribution evolution (Softmax as Iter 0, subsequent recursive iterations sharpening the peak). Right: Entropy reduction over recursive iterations compared to initial Softmax entropy.

5.2.3 Results

Iterating Eq. 2 significantly sharpens the distribution beyond the initial Softmax result, with entropy decreasing monotonically at each step (Fig. 6).

5.2.4 Analysis

This demonstrates how recursive amplification via Eq. 2 acts as an iterative sharpener. It could potentially replace or augment Softmax where dynamic control over distribution focus or hardware suitability of simple iterations is desired.

5.3 Implications for AI

The recursive feedback mechanism (modeled by Eq. 2 here) offers a different paradigm for activation or attention: tunable "decisiveness" via iterations, potential advantage for low-power hardware, inspiration for recurrent attention mechanisms [33]. Conceptually, it bears resemblance to dynamics in energy-based models [22] where iterations implicitly minimize an energy function, or attractor networks [19].

6 Discussion and Conclusion

6.1 Summary of Hypothesis and Findings

The Mutual Awakening Hypothesis (MAH) posits quantum collapse as an intrinsic, deterministic process driven by recursive, entropy-stabilizing feedback. We explored this using:

1. A simplified probability operator (Eq. 2), demonstrating bias-driven collapse (Exp 3.2), locality-preserving correlation propagation (Exp 3.3), adaptive selection (Exp 3.4), and self-organized instability (Exp 3.5).
2. More fundamental simulations on quantum states, confirming collapse via direct amplitude feedback (Exp 3.6), exploring dynamic entanglement evolution under simulated local feedback (Exp 3.7), showing robustness and complementarity with decoherence (Exp 3.8), and demonstrating tunable collapse rates via feedback strength (Exp 3.9).

Furthermore, the MAH principle, particularly via Eq. 2, inspired practical gradient-free classification algorithms (Sec 4) and an alternative iterative mechanism to Softmax in AI (Sec 5).

6.2 Implications for Quantum Foundations

MAH offers a potential observer-independent, continuous mechanism for state reduction, treating collapse as self-organization driven by inherent nonlinear dynamics, distinct from standard linear evolution [24]. It differs from explicit dynamical reduction models like GRW, CSL, or Diosi-Penrose [14, 25, 10, 26, 4] by emphasizing internal feedback rather than stochastic noise or gravitational effects as the primary driver. It provides a *selective* mechanism that complements decoherence (which suppresses interference [37, 30]) to explain the emergence of definite outcomes from quantum possibilities, avoiding the ontological commitments of Many-Worlds [13] or standard Bohmian mechanics [8]. The MAH process could be viewed as describing the transition from a decohered mixture to a single outcome, effectively completing the measurement process potentially initiated by decoherence.

6.3 Implications for Thermodynamics

The focus on Shannon entropy reduction [32], related to the more general von Neumann entropy [34, 35], links quantum collapse to thermodynamic principles of self-organization and information

processing [17, 28], suggesting measurement might be viewed as a system actively minimizing its informational uncertainty, perhaps related to Landauer’s principle on the thermodynamic cost of information erasure [21].

6.4 Implications for Quantum and Classical Computation

- **QML:** Motivates gradient-free approaches (e.g., Sec 4 using Eq. 2), potentially valuable for NISQ hardware [27, 7]. The amplitude-level feedback concepts (Sec 3.6-3.9) might inspire deeper quantum algorithms [31, 9].
- **Classical AI:** Offers iterative alternatives (e.g., Sec 5 using Eq. 2) to standard activation/attention functions like Softmax [16, 33], possibly enabling dynamic control and efficient hardware implementations, resonating with neuromorphic computing concepts [23].

6.5 Limitations and Future Work

This work presents initial formulations and validations. Key future directions include:

- **Theoretical Foundation:** Develop a rigorous derivation of the amplitude feedback dynamics (Sec 3.6-3.9) from first principles (e.g., modified quantum field theory or nonlinear Schrödinger equations [6]). Clarify the physical origin and nature of the feedback parameters (γ, k, b_i). Establish a formal link between the amplitude dynamics and the effective probability model (Eq. 2). Explore connections to and distinctions from existing objective collapse models [4].
- **Entanglement Dynamics:** Rigorously analyze the locality and signaling properties of MAH-like feedback in multipartite systems (extending Exp 3.7), ensuring compatibility with Bell’s theorem [5] and experimental results [3]. Develop and justify physically sound feedback operators for entangled states. The specific $U \otimes I$ operator used in Exp 3.7 requires deeper theoretical backing or replacement.
- **Decoherence Interaction:** Model the interplay between environmental decoherence [37, 30] and MAH feedback more comprehensively, exploring different noise models (e.g., non-Markovian effects) and system-environment coupling scenarios (extending Exp 3.8).
- **Experimental Signatures:** Identify potential experimental regimes where subtle deviations predicted by MAH might be observable compared to standard QM + decoherence. Could deviations appear in high-precision tests in mesoscopic systems [2], complex cavity QED setups, optomechanical systems, or via weak measurement protocols [1] that aim to probe system dynamics with minimal disturbance?
- **Computational Applications:** Thoroughly evaluate the performance, scalability, and robustness of MAH-inspired algorithms (Sec 4, 5) on complex, high-dimensional, real-world datasets. Explore the development of hybrid quantum-classical algorithms where MAH dynamics could play a role in state preparation, error mitigation, or measurement result refinement on near-term quantum devices.

Conclusion

The Mutual Awakening Hypothesis, explored here through both probability-level and amplitude-level simulations, offers a compelling conceptual framework for understanding quantum collapse as an intrinsic, recursive, and entropy-stabilizing process. Our results support its core tenets

and highlight its potential to bridge quantum foundations [24] with thermodynamics and inspire novel computational methods. While significant theoretical and experimental work remains, MAH provides a potentially unifying perspective on measurement, self-organization, and learning in the quantum realm.

References

References

- [1] Aharonov, Y., Albert, D. Z., & Vaidman, L. (1988). How the result of a measurement of a component of the spin of a spin-1/2 particle can turn out to be 100. *Physical Review Letters*, 60(14), 1351–1354.
- [2] Arndt, M., & Hornberger, K. (2014). Testing the limits of quantum mechanics: motivation, state of play, prospects. *Nature Physics*, 10(4), 271–277.
- [3] Aspect, A., Dalibard, J., & Roger, G. (1982). Experimental test of Bell's inequalities using time-varying analyzers. *Physical Review Letters*, 49(25), 1804–1807.
- [4] Bassi, A., Lochan, K., Satin, S., Singh, T. P., & Ulbricht, H. (2013). Models of Wave-Function Collapse, Underlying Mechanisms, and Experimental Tests. *Reviews of Modern Physics*, 85(2), 471–527.
- [5] Bell, J. S. (1964). On the Einstein Podolsky Rosen paradox. *Physics Physique Fizika*, 1(3), 195–200.
- [6] Bialynicki-Birula, I., & Mycielski, J. (1976). Nonlinear wave mechanics. *Annals of Physics*, 100(1-2), 62–93.
- [7] Biamonte, J., Wittek, P., Pancotti, N., Rebentrost, P., Wiebe, N., & Lloyd, S. (2017). Quantum machine learning. *Nature*, 549(7671), 195–202.
- [8] Bohm, D. (1952). A suggested interpretation of the quantum theory in terms of "hidden" variables. I & II. *Physical Review*, 85(2), 166–193.
- [9] Cerezo, M., Arrasmith, A., Babbush, R., Benjamin, S. C., Endo, S., Fujii, K., ... & Coles, P. J. (2021). Variational quantum algorithms. *Nature Reviews Physics*, 3(9), 625–644.
- [10] Diósi, L. (1989). Models for universal reduction of macroscopic quantum fluctuations. *Physical Review A*, 40(3), 1165–1174.
- [11] Dirac, P. A. M. (1958). *The Principles of Quantum Mechanics*, 4th Edition. Oxford University Press.
- [12] Elman, J. L. (1990). Finding structure in time. *Cognitive Science*, 14(2), 179–211.
- [13] Everett III, H. (1957). 'Relative state' formulation of quantum mechanics. *Reviews of Modern Physics*, 29(3), 454–462.
- [14] Ghirardi, G. C., Rimini, A., & Weber, T. (1986). Unified dynamics for microscopic and macroscopic systems. *Physical Review D*, 34(2), 470–491.
- [15] Gisin, N. (1998). Quantum cloning without signaling. *Physics Letters A*, 242(1-2), 1–3.
- [16] Goodfellow, I., Bengio, Y., & Courville, A. (2016). *Deep Learning*. MIT Press.
- [17] Haken, H. (1975). Cooperative phenomena in systems far from thermal equilibrium and in nonphysical systems. *Reviews of Modern Physics*, 47(1), 67–121.

- [18] Haken, H. (1983). *Synergetics: An Introduction. Nonequilibrium Phase Transitions and Self-Organization in Physics, Chemistry and Biology*, 3rd Edition. Springer-Verlag.
- [19] Hopfield, J. J. (1982). Neural networks and physical systems with emergent collective computational abilities. *Proceedings of the National Academy of Sciences*, 79(8), 2554–2558.
- [20] Kohonen, T. (1990). The self-organizing map. *Proceedings of the IEEE*, 78(9), 1464–1480.
- [21] Landauer, R. (1961). Irreversibility and heat generation in the computing process. *IBM Journal of Research and Development*, 5(3), 183–191.
- [22] LeCun, Y., Chopra, S., Hadsell, R., Ranzato, M., & Huang, F. (2006). A tutorial on energy-based learning. In *Predicting structured data* (pp. 1–50). MIT Press.
- [23] Mead, C. (1990). Neuromorphic electronic systems. *Proceedings of the IEEE*, 78(10), 1629–1636.
- [24] Nielsen, M. A. & Chuang, I. L. (2010). *Quantum Computation and Quantum Information*, 10th Anniversary Edition. Cambridge University Press.
- [25] Pearle, P. (1989). Combining stochastic dynamical state-vector reduction with spontaneous localization. *Physical Review A*, 39(5), 2277–2289.
- [26] Penrose, R. (1996). On gravity’s role in quantum state reduction. *General Relativity and Gravitation*, 28(5), 581–600.
- [27] Preskill, J. (2018). Quantum Computing in the NISQ era and beyond. *Quantum*, 2, 79.
- [28] Prokopenko, M., Boschetti, F., & Ryan, A. J. (2009). An information-theoretic primer on complexity, self-organization, and emergence. *Complexity*, 15(1), 11–28.
- [29] Rumelhart, D. E., Hinton, G. E., & Williams, R. J. (1986). Learning internal representations by error propagation. In D. E. Rumelhart, J. L. McClelland, & the PDP Research Group (Eds.), *Parallel distributed processing: Explorations in the microstructure of cognition. Vol. 1: Foundations* (pp. 318–362). MIT Press.
- [30] Schlosshauer, M. A. (2007). *Decoherence: and the quantum-to-classical transition*. Springer Science & Business Media.
- [31] Schuld, M. & Petruccione, F. (2018). *Supervised Learning with Quantum Computers*. Springer.
- [32] Shannon, C. E. (1948). A mathematical theory of communication. *The Bell System Technical Journal*, 27(3), 379–423.
- [33] Vaswani, A., Shazeer, N., Parmar, N., Uszkoreit, J., Jones, L., Gomez, A. N., Kaiser, Ł., & Polosukhin, I. (2017). Attention is all you need. *Advances in Neural Information Processing Systems (NeurIPS)*, 30.
- [34] Von Neumann, J. (1955). *Mathematical Foundations of Quantum Mechanics*. (R. T. Beyer, Trans.). Princeton University Press.
- [35] Wehrl, A. (1978). General properties of entropy. *Reviews of Modern Physics*, 50(2), 221–260.
- [36] Zurek, W. H. (1981). Pointer basis of quantum apparatus: Into what mixture does the wave packet collapse? *Physical Review D*, 24(6), 1516–1525.

- [37] Zurek, W. H. (2003). Decoherence, einselection, and the quantum origins of the classical. *Reviews of Modern Physics*, 75(3), 715–775.